

Hyperoxic Reperfusion after Global Cerebral Ischemia Promotes Inflammation and Long-Term Hippocampal Neuronal Death

Julie L. Hazelton,^{1,2} Irina Balan,^{1,2} Greg I. Elmer,³ Tibor Kristian,^{1,2} Robert E. Rosenthal,^{1,2,4} Gary Krause,⁵ Thomas H. Sanderson,⁵ and Gary Fiskum^{1,2}

Abstract

In this study we tested the hypothesis that long-term neuropathological outcome is worsened by hyperoxic compared to normoxic reperfusion in a rat global cerebral ischemia model. Adult male rats were anesthetized and subjected to bilateral carotid arterial occlusion plus bleeding hypotension for 10 min. The rats were randomized to one of four protocols: ischemia/normoxia (21% oxygen for 1 h), ischemia/hyperoxia (100% oxygen for 1 h), sham/normoxia, and sham/hyperoxia. Hippocampal CA1 neuronal survival and activation of microglia and astrocytes were measured in the hippocampi of the animals at 7 and 30 days post-ischemia. Morris water maze testing of memory was performed on days 23–30. Compared to normoxic reperfusion, hyperoxic ventilation resulted in a significant decrease in normal-appearing neurons at 7 and 30 days, and increased activation of microglia and astrocytes at 7, but not at 30, days of reperfusion. Behavioral deficits were also observed following hyperoxic, but not normoxic, reperfusion. We conclude that early post-ischemic hyperoxic reperfusion is followed by greater hippocampal neuronal death and cellular inflammatory reactions compared to normoxic reperfusion. The results of these long-term outcome studies, taken together with previously published results from short-term experiments performed with large animals, support the hypothesis that neurological outcome can be improved by avoiding hyperoxic resuscitation after global cerebral ischemia such as that which accompanies cardiac arrest.

Key words: astrocyte; cardiac arrest; hippocampus; microglia; Morris water maze; resuscitation

Introduction

VARIOUS LINES OF EVIDENCE INDICATE that brain injury following global cerebral ischemia is exacerbated by hyperoxia during early stages of reperfusion. Hyperoxic reperfusion exacerbates brain lipid oxidation and protein oxidation (Liu et al., 1998; Mickel et al., 1987; Richards et al., 2006; Vereczki et al., 2006). In contrast to the concept that provision of high oxygen after global ischemia should promote aerobic energy metabolism, hyperoxic reperfusion elevates brain lactate, impairs metabolism of glucose to aerobic energy metabolites, and worsens the post-ischemic oxidized shift in tissue redox state (Feng et al., 1998; Liu et al., 1998; Mickel et al., 1987; Richards et al., 2007). Hyperoxic resuscitation also promotes damage to white matter in gerbils (Mickel et al., 1990), and hippocampal

neuronal death in dogs (Balan et al., 2006; Vereczki et al., 2006). On a neurological level, hyperoxia increases 14-day mortality in gerbils (Mickel et al., 1987), and worsens 12- to 24-h neurological outcome in dogs (Balan et al., 2006; Vereczki et al., 2006; Zwemer et al., 1994). In contrast to the deleterious effects of early hyperoxic reperfusion after global cerebral ischemia, hyperoxia may prove beneficial for focal cerebral ischemia (stroke) and certain forms of traumatic brain injury due to prolonged hypoperfusion and associated tissue hypoxia (Singhal et al., 2005; Tolia et al., 2004).

Comparisons of the effects of hyperoxic and normoxic reperfusion on neurochemical, histological, and neurological outcome in the gerbil global ischemia and the dog cardiac arrest models raise serious questions about the typical clinical practice of using 100% ventilatory oxygen (FIO₂) for cardiac arrest victims during CPR, and for prolonged periods

¹Department of Anesthesiology, ²Center for Shock, Trauma, and Anesthesiology Research, and ³Department of Psychiatry, Maryland Psychiatric Research Center, and ⁴Program in Trauma, Department of Emergency Medicine, University of Maryland School of Medicine, Baltimore, Maryland.

⁵Department of Emergency Medicine, Wayne State University School of Medicine, Detroit, Michigan.

following resuscitation (Balan et al., 2006). Nevertheless, considering the failure of numerous interventions in clinical trials for ischemic brain injury that were proven effective in animal models (Liebeskind et al., 2001), caution should be taken when interpreting the animal data. While normoxia appeared to reduce white matter damage in gerbils at 14 days of reperfusion, this finding was not quantified (Mickel et al., 1990). A highly quantitative and non-biased stereologic approach was used to demonstrate reduced hippocampal neuronal death in the clinically more relevant canine cardiac arrest model (Balan et al., 2006; Liu et al., 1998; Vereczki et al., 2006); however, these results were obtained at 24 h of reperfusion, while cell death continues for days to weeks following transient global cerebral ischemia. To test for the potential long-term benefits of normoxic resuscitation after global cerebral ischemia in an additional species, we examined longer-term hippocampal neuronal survival (at 7 and 30 days), and behavioral outcomes (at 23–30 days), using a rat model of transient global cerebral ischemia. Moreover, we quantified the persistent activation of microglia and astrocytes that occurs in this model. Our findings indicate that normoxic resuscitation improves long-term neuronal survival at both 7 and 30 days. Neurological outcome was significantly worse following hyperoxic, but not normoxic, resuscitation, compared to non-ischemic controls. Normoxic resuscitation also reduced cellular inflammatory reactions at 7, but not 30, days of reperfusion.

Methods

Animal experimental groups

Adult male Fisher 344 rats (300–400 g; Charles River Laboratories, Wilmington, MA) were maintained on a 12-h light/dark cycle with access to food and water *ad libitum*. Immediately prior to induction of ischemia, the rats were randomized to one of four resuscitation protocols for 7-day outcomes: sham/normoxic (sham + 21% FIO_2 for 1 h; $n = 4$), sham/hyperoxic (sham + 100% FIO_2 ; $n = 4$), ischemic/normoxic (ischemia + 21% FIO_2 ; $n = 8$), or ischemic/hyperoxic (ischemia + 100% FIO_2 ; $n = 8$); and for 30-day outcomes: sham/normoxic (sham + 21% FIO_2 for 1 h; $n = 5$), sham/hyperoxic (sham + 100% FIO_2 ; $n = 5$), ischemic/normoxic (ischemia + 21% FIO_2 ; $n = 10$), or ischemic/hyperoxic (ischemia + 100% FIO_2 ; $n = 10$). The rats were allowed to recover for 7 or 30 days, with water maze testing only for the animals in the experimental groups surviving 30 days. Only one animal was excluded from the study due to death during the surgical procedure and a substitute was included in the randomization. Bilateral hippocampal damage is typically observed using this model of global cerebral ischemia; however, three animals exhibited unilateral injury and were excluded from the study and not replaced (two normoxic 7-day post-ischemia and one hyperoxic 7-day post-ischemia). The experiments were carried out in accordance with the rules and regulations set forth by the University of Maryland regarding the care and use of animals under a protocol approved by the institution's animal care and use committee.

Surgery

Transient global cerebral ischemia was induced using the two-vessel occlusion plus hypotension technique originally described by Smith and colleagues (1984), and modified by

Sugawara and associates (2002). Anesthesia was induced with 5% halothane and maintained throughout surgery at 1.0–1.5% delivered via an endotracheal tube connected to a small animal ventilator (Harvard Apparatus, Holliston, MA) at a ventilatory rate of 75/min and tidal volume of 2.5 mL. Core temperature was measured and maintained at $37 \pm 0.5^\circ\text{C}$ using a homoeothermic blanket system (Harvard Apparatus). The right femoral artery was isolated and catheterized with PE50 tubing to allow continuous recording of arterial blood pressure, delivery of heparin (30 U), induction of hypotension by removal of blood, and collection of blood samples. Both common carotid arteries were exposed and isolated with loose ligatures through a midline cervical incision. Arterial blood gases were measured prior to the induction of ischemia and ventilatory parameters were adjusted to maintain PCO_2 and PO_2 within normal limits of 30.0–40.0 mm Hg and 80–100 mm Hg, respectively. Global ischemia was induced by clamping the common carotid arteries bilaterally and concurrently withdrawing blood into a heparinized syringe to maintain mean arterial pressure between 31 and 35 mm Hg for 10 min. During the ischemic interval, shed blood was maintained at 37°C . Immediately following the ischemic interval, the clamps were removed, blood was returned via the femoral artery catheter, and oxygen levels were adjusted to either a normoxic or hyperoxic resuscitation protocol. For normoxic resuscitation, the rats were maintained on a ventilator receiving input from an air tank (21% oxygen) for 1 h. For hyperoxic resuscitation, the rats were ventilated from a tank containing 100% oxygen for 1 h. All rats remained anesthetized under 1.5% halothane during ischemia and the designated resuscitation protocol.

In sham-operated rats, the femoral arteries were catheterized to allow blood sampling, but hypotension was not induced. Additionally, carotid arteries were isolated but not clamped. Arterial blood gases were measured prior to, and 10 and 60 min after, the induction of ischemia for all treatment groups. Anesthesia and hyperoxia were terminated 1 h post-experimental or sham ischemia. All animals were successfully extubated within 10 min following termination of anesthesia. The rats recovered full consciousness in a clean pre-warmed cage and were then moved back to their home cages.

Morris water maze

The water maze consists of a fiberglass circular pool (1.6 m in diameter and 60 cm high). The pool was filled to a depth of 32 cm with tap water made opaque by non-toxic white paint and maintained at $26 \pm 1.0^\circ\text{C}$. A translucent acrylic platform (12 cm) was placed inside the pool, 30 cm from the pool wall. The room contained numerous visual cues, in the form of colored shapes, located outside of the maze on the room walls and room partition. A video camera was mounted from the ceiling directly above the pool and connected to a computer running a software package that tracks and records the path taken by the rat. The rats were permitted to recover for 3 weeks following induction of ischemia prior to the onset of behavioral testing in the water maze. Because the monitoring software tracks movement by color contrast, a black triangle was added to the top of each rat's head with permanent hair color prior to habituation and testing. The rats were habituated to the pool on the day prior to the onset of behavioral testing by allowing them to swim for 2 min.

Behavioral testing occurred over 7 days and consisted of three consecutive phases: (1) hidden platform training (4 days), (2) probe testing (1 day), and (3) visible platform testing (2 days). The rats were lowered into the maze facing pool-side from each of the four start locations (north, south, east, and west) each day of testing. Between each swim trial, the rats were returned to dry, pre-warmed cages and allowed to rest. The location of the platform remained the same for all phases.

Spatial learning and navigation were evaluated in the hidden platform training phase in which the rats were given 2 min per swim to find the platform located 1.5 cm under the surface of the water. Upon reaching the platform, latency was recorded and the rats were permitted to remain on the platform for an additional 30 sec. Subjects who failed to find the platform within 2 min were gently guided by hand to the platform and allowed to remain there for an additional 30 sec.

The degree to which the rat learned the spatial location of the platform was determined during a probe test. During this test the platform was removed and the rats were again lowered into the maze from each of the four start locations. The rats were given 60 sec to swim freely during each of the four trials. The establishment of place learning strategy is inferred from this type of trial if the rat spends more time in the target quadrant than the non-target quadrants (Skelton, 1998).

In the visible platform testing phase of testing, the rats were given 60 sec per swim to find the platform located 1.5 cm above the surface of the water. Upon reaching the platform, latency was recorded and the rats were permitted to remain on the platform for an additional 30 sec. This task is viewed as a control procedure to reveal deficits in sensory, motor, or motivational processes (Skelton, 1998).

Tissue preparation

At the end of the appropriate experimental period (7 or 30 days), the rats were anesthetized with ketamine and transcardially perfused with 4% paraformaldehyde plus 2.5% acrolein at either 7 or 30 days post-surgery. The brains were removed from the skulls and transferred into 30% sucrose. Once the brains sank to the bottom of the container, they were cut (30 μ m) on a freezing sliding microtome, yielding 24 series per animal and kept in cryoprotectant (-20° C) until further processing was initiated (Watson et al., 1986).

Histopathology

Representative sections throughout the hippocampus (1 in 12 series, six sections total) were collected and stained with cresyl violet. The sections were placed sequentially in 50%, 75%, and 95% ethanol for 5 min each, and then in 100% ethanol for 6 h. The sections were then rehydrated in 95%, 75%, and 50% ethanol and water for 5 min each, and treated with cresyl violet solution (FD NeuroTechnologies, Baltimore, MD) for 2 min. The slides were then placed in 0.1% acetic acid in 75% ethanol for 2 min, rinsed in water, dehydrated, and mounted on cover-slips with DPX. Using Stereo Investigator software (MicroBrightField, Williston, VT), unbiased estimates of the total number of uninjured neurons in the CA1 region were obtained using the optical fractionator technique of stereology. After outlining the boundaries of the CA1 region at low magnification (10 \times), the software places a set of optical disector frames (count frame 30 \times 30 μ m) in a systematic-

random fashion. Shrunken neurons with a condensed nucleus and lacking a nucleolus were classified as injured and/or dying cells. Non-injured neurons were then counted in optical dissectors to 7 μ m in depth at 100 \times magnification (West et al., 1991). At least 500 cells were sampled to ensure robustness of the data (Schmitz and Hof, 2000).

Immunohistochemistry

Adjacent series of free-floating sections were single-labeled with antibodies against glial fibrillary acidic protein (GFAP) and ionized calcium binding adaptor protein-1 (Iba-1) by rinsing multiple times in 0.05 M KPBS buffer before and after exposure to the following: 1% solution of sodium borohydride for 20 min; primary antibody diluted in 0.05 M KPBS + 0.4% Triton-X for 48 h (anti Iba-1 [microglia] 1:70K; Wako Diagnostics, Richmond, VA, or anti-GFAP [astrocytes] 1:150K; Dako North America, Inc., Carpinteria, CA); secondary antibody diluted in 0.05 M KPBS + 0.4% Triton-X 1:600 for 1 h; and incubation in A/B solution (1:222) for 1 h. The tissues were then rinsed before and after 12 min of incubation in Ni-DAB solution with 0.175 M sodium acetate buffer. After a final rinse in KPBS buffer, the slices were mounted on slides, dehydrated, and cover-slipped with DPX mounting media. For qualitative imaging only, a subset of tissue was stained for fluorescent images of astrocytes (1:30K) and microglia (1:9K) using the same primary antibodies listed above, and a fluorescent tagged secondary antibody (1:500; Invitrogen Corp., Carlsbad, CA). The sections were examined with a Nikon Eclipse E800 microscope equipped with appropriate filters for the fluorochrome-treated sections.

Quantification of microglia and astrocyte activation

Representative sections throughout the hippocampus (1 in 12 series, six sections total) were processed with antibodies against Iba-1 and GFAP using a Ni-DAB chromogen solution, which results in a black insoluble deposit at the site of the antigen. Using Stereo Investigator software, unbiased estimates of the total number of morphologically distinct glial cells in the CA1 region were obtained using the optical fractionator technique of stereology, as previously described.

Hippocampal microglial cells were classified into three categories, based on subjective visual inspection as described previously by Soltys and associates (2001). Cells with small, round bodies and abundant systems of regularly branched processes were classified as "resting" cells. Cells with larger and irregular cell bodies, and thicker and irregular processes were recognized as "hypertrophic" cells. The last category, designated as "activated," consisted of cells with either a few short, or no processes, and an irregular, amoeboid body.

GFAP-immunoreactive cells were classified into three categories: normal, moderate, and intensely activated astrocytes, based on morphological characteristics as assessed by subjective visual inspection. Astrocytes exhibiting small cell bodies and numerous thin, branched processes were classified as normal resting astrocytes, while those with hypertrophic cell bodies and numerous thick processes were deemed as moderately activated astrocytes. Astrocytes exhibiting substantially larger hypertrophic cell bodies and few short altered processes were classified as intensely "activated."

Data analysis

Physiological measurements and data obtained from histologic outcome measures were analyzed using a one-way analysis of variance (ANOVA) followed by the multiple comparison Student-Newman-Keuls method, with $p < 0.05$ considered statistically significant. Group sizes were $n = 6-8$ /group for 7-day outcome, and $n = 10$ /group for 30-day outcome.

Data obtained for behavior from the Morris water maze tests were analyzed in several ways. In order to determine if there was an interaction between ischemia and the level of ventilatory oxygen during resuscitation, a three-way repeated-measures ANOVA was conducted on the training data (ischemia \times oxygenation with training day as a repeated measure), while a two-way ANOVA (ischemia \times oxygenation) was conducted on the probe trial data. The visible platform test was analyzed using a two-way ANOVA with treatment (ischemia \times oxygenation) as a between-subjects variable, and test day as a within-subjects repeated measure. The relationship between spatial learning capacity and total number of neurons in the CA1 region was assessed using Pearson's product-moment correlation.

Results

Physiological variables

Physiological variables measured prior to and 60 min after 10 min global cerebral ischemia were compared across sham and ischemia reperfusion groups (Table 1). No significant differences in pre-ischemic values for arterial blood pressure, pH, P_{CO_2} , P_{O_2} , glucose, rectal temperature, or weight were observed. A temperature probe was also inserted into the frontalis muscle of a subset of animals to verify that both scalp and body temperatures remained within $37 \pm 0.5^\circ\text{C}$. At 60 minutes post-ischemia, the P_{O_2} values for hyperoxic (sham and ischemic) animals were significantly ($>400\%$) greater than those of the normoxic (sham and ischemic) groups, as expected. No differences among groups were found for any other physiological parameters. In addition, no differences were found between groups for body weight prior to ischemia or later, at the time of perfusion (data not shown).

Hippocampal neuronal death

Stereologic quantification of normal-appearing pyramidal neurons throughout the CA1 hippocampal subfield of four normoxic sham and four hyperoxic sham animals at 7 days after the sham procedures revealed no significant differences between the two non-ischemic sham groups. The same analysis for five each of normoxic and hyperoxic sham rats at 30 days post-ischemia also revealed no differences. These groups were then pooled to generate $n = 8$ shams for the 7-day outcome time point, and $n = 10$ shams for the 30-day outcome time point. At 7 days there was a significant (33%) reduction in neuronal survival for the normoxic reperfusion group compared to the pooled shams ($p < 0.01$), and a significant (64%) reduction in the hyperoxic reperfusion group compared to the pooled shams ($p < 0.001$), also resulting in a significant (45%) reduction in neuronal survival for hyperoxic compared to normoxic reperfusion ($p < 0.05$). At 30 days post-ischemia, there were significant and greater reductions in neuronal survival for both the normoxic and hyperoxic reperfusion groups (64% and 82%, respectively), compared to shams ($p < 0.001$), and a persistent, significantly lower rate (50%) of neuronal survival with hyperoxic compared to normoxic reperfusion ($p < 0.05$; Fig. 1).

Activation of microglia and astrocytes

Figure 2A provides examples of fluorescent images of Iba-1-immunoreactive microglia within the hippocampi of 7-day shams and 7-day reperfusion following either normoxic or hyperoxic resuscitation. Figure 2B and C provide the stereologic quantification of resting, hypertrophic, and activated microglia within the CA1 subregion as performed by an observer blinded to sample identification. Iba-1-immunoreactive cells stained with Ni-DAB were classified based on the shapes of their cell bodies and the number and shape of cell processes as described in the methods section. Almost all Iba-1-stained microglia observed in the hippocampi from pooled sham animals were categorized as resting. In contrast, very few resting microglia were observed in samples from either the ischemia/normoxic or hyperoxic groups at either 7 or 30 days of reperfusion. In contrast to the paucity of activated microglia observed in the 7- or 30-day shams, an abundance of activated microglia were observed in both ischemia/reperfusion groups

TABLE 1. PHYSIOLOGIC VARIABLES PRIOR TO AND 60 MIN AFTER GLOBAL ISCHEMIA FOR SHAM-OPERATED AND ISCHEMIC ANIMALS UNDER NORMOXIC AND HYPEROXIC RESUSCITATION

	Sham normoxic		Sham hyperoxic		Ischemic normoxic		Ischemic hyperoxic	
	Pre	60 min post	Pre	60 min post	Pre	60 min post	Pre	60 min post
BP (mm Hg)	101 \pm 8	85 \pm 6	96 \pm 8	86 \pm 8	95 \pm 5	87 \pm 4	102 \pm 5	89 \pm 4
pH	7.451 \pm 0.016	7.443 \pm 0.016	7.455 \pm 0.016	7.425 \pm 0.013	7.466 \pm 0.013	7.419 \pm 0.012	7.450 \pm 0.009	7.361 \pm 0.039
P_{CO_2} (mm Hg)	35.8 \pm 2.0	35.7 \pm 2.7	36.1 \pm 1.9	39.1 \pm 1.7	35.9 \pm 1.2	39.4 \pm 1.4	35.9 \pm 1.3	41.7 \pm 1.9
P_{O_2} (mm Hg)	96.1 \pm 5.6	91.0 \pm 6.1	90.0 \pm 3.5	487.6 \pm 33.5*	92.2 \pm 3.2	85.7 \pm 3.5	93.9 \pm 3.8	486.1 \pm 22.1*
Glucose (mg/dL)	139 \pm 6	121 \pm 8	147 \pm 14	121 \pm 5	150 \pm 7	123 \pm 8	143 \pm 7	119 \pm 5
Temperature ($^\circ\text{C}$)	37.1 \pm 0.1	37.1 \pm 0.1	36.9 \pm 0.1	37.1 \pm 0.1	37.1 \pm 0.1	37.0 \pm 0.1	37.0 \pm 0.1	37.2 \pm 0.1

* $p < 0.001$ compared to both pre-ischemic or pre-sham ischemic and compared to 60 min post-ischemia/normoxia, or post-sham ischemia/normoxia.

Values for animals used for both 7-day and 30-day outcomes were pooled and represent the means \pm standard error for $n = 16-18$ animals per group.

BP, blood pressure; P_{CO_2} , partial carbon dioxide pressure; P_{O_2} , partial oxygen pressure.

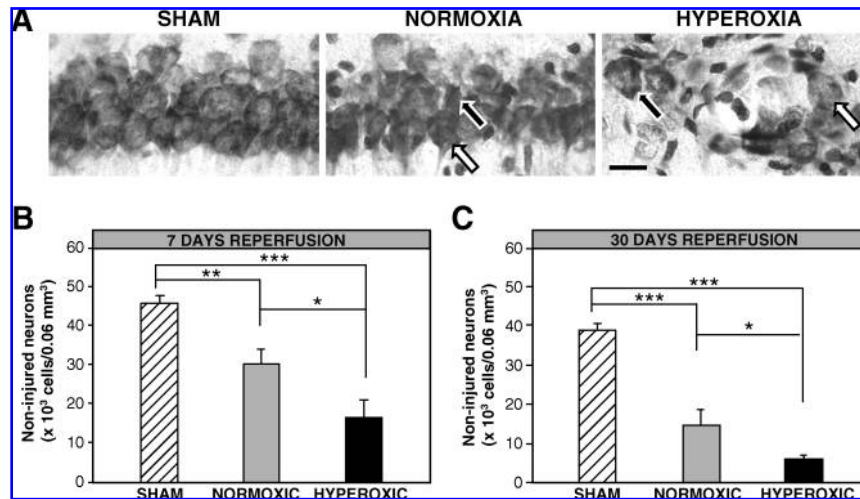


FIG. 1. Promotion of hippocampal neuronal death by hyperoxic reperfusion after global cerebral ischemia. Rats were perfusion-fixed at 7 days (**B**) and 30 days (**C**) reperfusion after 10-min global cerebral ischemia was induced by bilateral carotid artery occlusion and bleeding hypotension. Normal-appearing neurons in the CA1 subregion were quantified using a stereological approach on cresyl violet-stained sections, as exemplified by the images shown in **A**, which were generated from the brains from animals perfusion-fixed at 30 days reperfusion. Examples of neurons exhibiting normal and abnormal morphologies are shown by the white and black arrows, respectively (scale bar = 25 μ m; values represent the means \pm standard error for $n = 6-8$ animals per group [7 days], and $n = 10$ per group [30 days]; * $p < 0.05$, ** $p < 0.01$, *** $p < 0.001$).

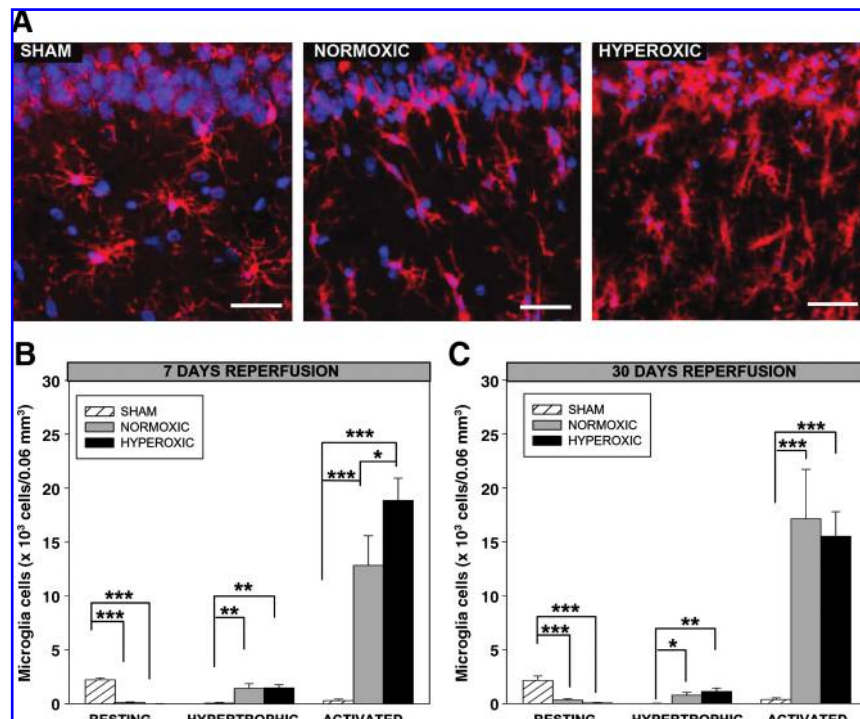


FIG. 2. Microglial activation in the hippocampal CA1 subregion following global cerebral ischemia. Rats were perfusion-fixed at 7 days (**B**) and 30 days (**C**) reperfusion after 10 min of global cerebral ischemia. Sections were then stained using Hoechst (blue) and primary antibody to Iba-1 (red) and visualized using fluorescent immunodetection (**A**), or using nickel-3,3'-diaminobenzidine (Ni-DAB), for stereologic quantification (**B** and **C**). Ionized calcium binding adaptor protein-1 (Iba-1)-immunoreactive cells were classified as resting, hypertrophic, or activated (scale bars for images obtained at 20 \times magnification = 25 μ m; values represent the means \pm standard error for $n = 6-8$ animals per group [7 days], and $n = 9-10$ animals per group [30 days]; * $p < 0.05$, ** $p < 0.01$, *** $p < 0.001$). Color image is available online at www.liebertonline.com/neu.

at both periods of reperfusion, with a significantly greater (38%) level of microglial activation in hyperoxic compared to normoxic animals at 7 days reperfusion ($p < 0.05$), but no difference was observed at 30 days reperfusion. Activated microglia displaying large, amoeboid cell bodies and relatively few and short processes were often observed among and surrounding degenerating CA1 pyramidal neurons (Fig. 2A). In addition to resting and activated microglia, a significant increase in hypertrophic microglia were observed at 7 and 30 days of reperfusion, compared to shams ($p < 0.01$), with no difference between the normoxic and hyperoxic groups.

Figure 3A displays examples of fluorescent images of GFAP-immunoreactive astrocytes within the same CA1 region used for microglial quantification. The Ni-DAB-stained sections were used for quantification; astrocytes were classified as normal, or either moderately or intensely activated. A significant (>70%) reduction in normal-appearing astrocytes was observed following ischemia and either 7 or 30 days reperfusion, with no difference between the normoxic and hyperoxic groups. Intensely activated astrocytes were not present in any of the sham animals, yet a very large and significant increase in these cells was observed after ischemia and 7 or 30 days reperfusion in both the normoxic and hyperoxic animal groups ($p < 0.001$). While the number of intensely-activated astrocytes was no different between the normoxic and hyperoxic groups at 30 days reperfusion, there was a strong trend toward fewer activated cells in the

normoxic group at 7 days reperfusion ($p = 0.06$). Moderately-activated astrocytes were present in sham animals and both reperfusion groups at both 7 and 30 days reperfusion. Interestingly, while there were no significant differences among the groups at 30 days, the number of moderately-activated astrocytes in normoxic animals was significantly greater than in both the hyperoxic animals and the sham animals at 7 days reperfusion ($p < 0.01$).

Behavior

A number of dependent variables were collected during each phase of the behavioral assessment. The primary dependent measures used to assess performance in the water maze were latency (in seconds) to reach the platform, percentage of time in the target quadrant, and percentage of the travel path in the target quadrant. Additional dependent measures used to assess potential confounding variables unrelated to spatial navigation were speed during active movement and percentage of the travel path in thigmotaxis.

The results for the hidden platform training phase are shown in Figure 4A and C. Overall differences between the experimental groups were subtle. There was no overall main effect of oxygenation, ischemia, or an interaction between the two main factors on the latency to locate the platform across training days. There was a significant difference across training days between experimental groups that experienced ischemia versus those that did not as they learned to locate the

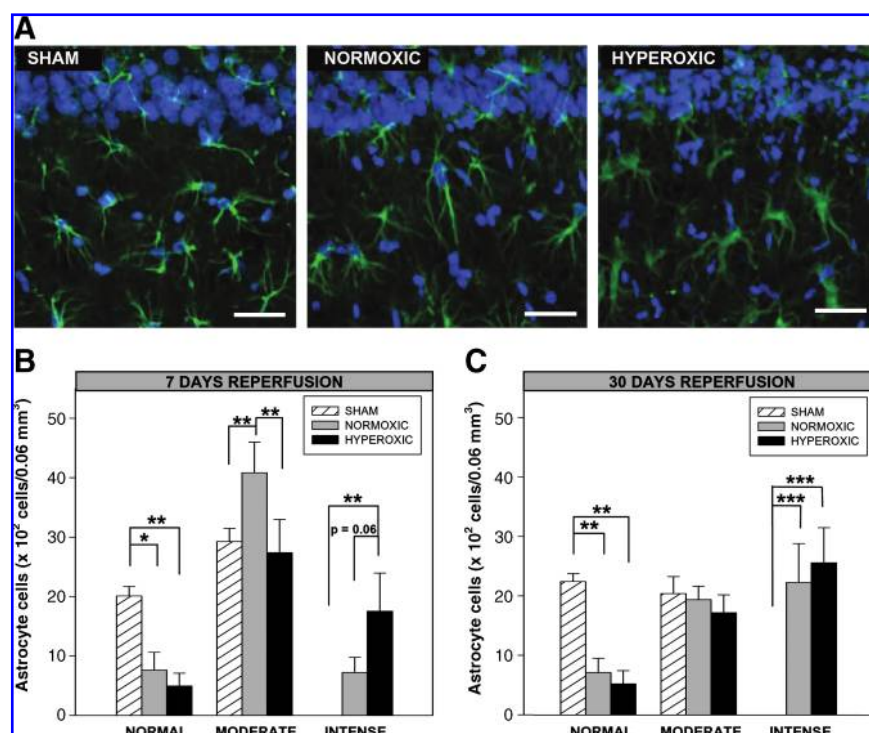


FIG. 3. Astrocyte activation in the hippocampal CA1 subregion following global cerebral ischemia. Rats were perfusion-fixed at 7 days (B) and 30 days (C) reperfusion after 10 min of global cerebral ischemia. Sections were then stained using Hoechst (blue) and primary antibody to glial fibrillary acidic protein (green) and visualized using fluorescent immunodetection (A), or nickel-3,3'-diaminobenzidine (Ni-DAB), for stereologic quantification (B and C). GFAP-immunoreactive cell activation was morphologically classified as normal, moderate, or intense (scale bars for images obtained at 20 \times magnification = 25 μ m; values represent the means \pm standard error for $n = 6-8$ animals per group [7 days], and 9-10 animals per group [30 days]; * $p < 0.05$, ** $p < 0.01$, *** $p < 0.001$). Color image is available online at www.liebertonline.com/neu.

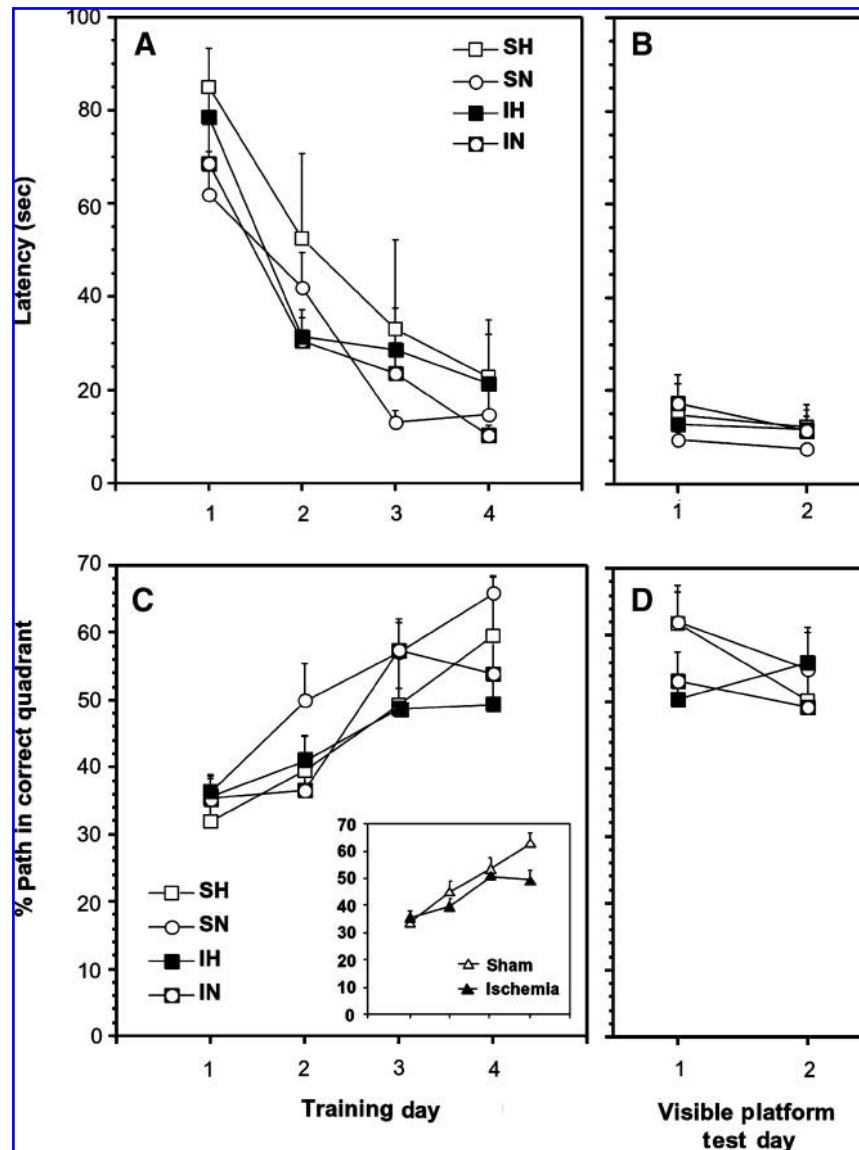


FIG. 4. Effects of global cerebral ischemia and normoxic and hyperoxic reperfusion on Morris water maze measures of learning and memory. Latency to reach the hidden platform and the percentage of the swim path in the target quadrant during training are shown in panels A and C, respectively. Results from the visible platform tests are provided in panels B and D, respectively. The insert in panel C shows the significant main interaction effect between sham versus ischemic experimental groups. Experimental groups were sham/hyperoxic (SH; $n = 5$), sham/normoxic (SN; $n = 5$), ischemic/hyperoxic (IH; $n = 10$), and ischemic/normoxic (IN; $n = 10$). Each point represents the mean \pm standard error.

hidden platform [ischemia \times training day: $F(3,23) = 2.96$; $p < 0.05$; Fig. 4B and insert in C]. The groups that were exposed to ischemic conditions spent less time in the target quadrant, especially near the end of the training period. There was no difference between groups in their active speed (m/sec) during the course of the training period. The latency to reach the target (Fig. 4B), and the percentage of the path in the target quadrant (Fig. 4D), did not differ significantly across experimental groups when the platform was clearly visible above the water.

A test of memory retention revealed an overall main effect of ischemia on the amount of time the subjects spent searching for the platform in the correct target quadrant (Fig. 5). Ischemia significantly decreased the amount of time the subjects

spent searching for the platform in the correct target quadrant [ischemia: $F(1,28) = 4.54$; $p < 0.04$]. There was no difference between the hyperoxic and normoxic sham-treated groups. When these two groups are combined, *post-hoc* contrast analysis reveals a significant difference between pooled sham subjects and the ischemic-hyperoxic [$F(1,26) = 5.90$, $p < 0.02$], but not the ischemic-normoxic groups ($p < 0.22$). There was no difference between groups in their active speed during the course of the training period.

The correlation between CA1 cell number and the percentage of time spent in the target quadrant during the probe test was statistically significant ($p < 0.047$) (data not shown). However, the relationship was not robust in that hippocampal cell number accounted for only about 15% of the variance

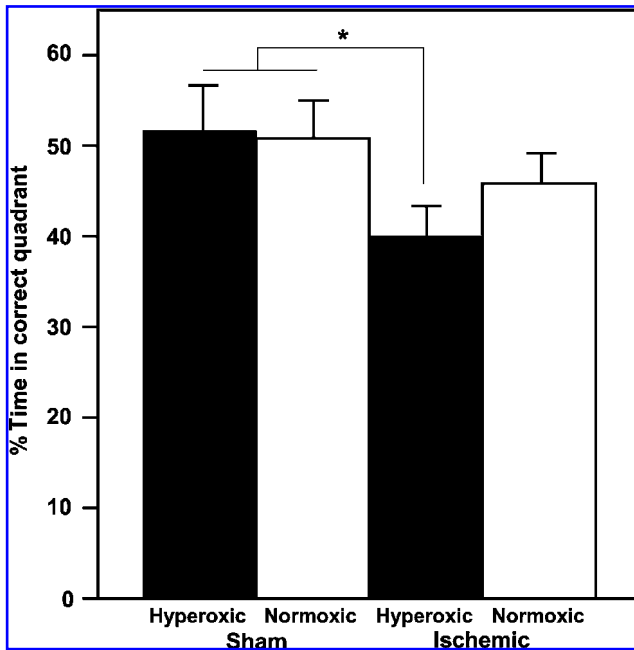


FIG. 5. Hyperoxic reperfusion reduces the percentage of time that post-ischemic rats spend searching for the platform in the correct quadrant during the probe test. Values represent the mean \pm standard error for sham/hyperoxic ($n=5$), sham/normoxic ($n=5$), ischemic/hyperoxic ($n=10$), and ischemic/normoxic ($n=10$; $*p < 0.05$).

in water maze performance during the probe test ($r^2=0.148$). Subjects with high cell numbers but poor performance throw off the correlation. Hippocampal cell number was not significantly correlated with any variable in the training or visible platform phase.

Discussion

The primary conclusion derived from this study is that significant short- and long-term protection against hippocampal neuronal death is achieved by avoiding hyperoxic reperfusion following transient global cerebral ischemia. The results of this study expand upon those we previously reported using a clinically relevant model of canine cardiac arrest and resuscitation, demonstrating that normoxic resuscitation reduces early oxidative modifications to lipids and proteins, improves cerebral energy metabolism, and improves both short-term neuronal survival and neurologic outcome (Balan et al., 2006; Liu et al., 1998; Richards et al., 2007; Vereczki et al., 2006). Hyperoxic resuscitation significantly exacerbated hippocampal CA1 neuronal death at 24 h in the canine model, and at 7 and 30 days in the rat model (Fig. 1). Our cardiac arrest studies used exclusively females, whereas the rat global ischemia experiments used exclusively males, suggesting that the deleterious effects of hyperoxic resuscitation are not gender-specific. Hyperoxia also substantially worsened neurological outcome at 23 h in the canine model, but caused only subtle neurologic impairment at days 23–27 in the rat model, which was significantly different from shams, but not from normoxic-reperfused ischemic rats (Fig. 5). The differences in the degree to which ventilatory

oxygen affects neurological outcome in the two models is most likely due to the differences in the extent of neuronal death throughout the brain in these two models, that both utilized 10 min of complete global cerebral ischemia. The canine cardiac arrest model is characterized by rapid and extensive neuronal death throughout all hippocampal subregions, several layers of the cortex, the Purkinje cell layer of the cerebellum, and in several additional locations (Rosenthal et al., 2003; Williams et al., 2006). In contrast, following 10 min of bilateral carotid occlusion plus bleeding hypotension in the rat, neuronal death is primarily limited to the CA1 subregion of the hippocampus and ventral regions of the thalamus, with relatively little neuropathology observed in other brain locations, including the cortex (Dietrich et al., 1993).

The fact that only subtle alterations in learning and memory were detected in the hyperoxic reperfused rats, despite the robust loss of viable CA1 neurons in these animals, is not entirely unexpected and is consistent with a report by Olsen and associates (1994), demonstrating similar correlation coefficients of <0.4 between surviving neurons and performance in the acquisition and probe tests. A longer duration of forebrain ischemia in the rat and more animals may be necessary to generate sufficient neurological impairment (which may include supporting brain regions), and power to detect significant differences in behavior between rats receiving hyperoxic and normoxic reperfusion. Regardless, preservation of neuronal cells is likely beneficial, and may be empirically revealed using a battery of tests designed to probe different demands placed on hippocampal function (Wishaw et al., 1994).

Another important conclusion reached in this study is that cellular inflammatory reactions, represented by activation of both microglia and astrocytes, are robust and persistent throughout at least 30 days of reperfusion. Furthermore, these reactions are significantly reduced by normoxic compared to hyperoxic reperfusion, when measured at 7 but not 30 days following ischemia (Figs. 2 and 3). While these cellular inflammatory responses are more commonly associated with focal cerebral ischemia (stroke), a comprehensive study by Sugawara and colleagues (2002) demonstrated extensive microglial activation that started as early as 1 day after 10-min global cerebral ischemia and persisted for at least 56 days. Although not specifically quantified, these investigators also reported astrocyte activation at reperfusion periods of 28 and 56 days that was qualitatively similar to what we documented at 30 days reperfusion (Fig. 3). Both microglia and astrocytes perform critical neuroprotective functions (e.g., provision of neurotrophic factors); however, the results of several studies indicate that when these cells are highly activated, they can also contribute to neuronal injury and death through several mechanisms (e.g., production of reactive oxygen and nitrogen species) (Hailer, 2008). It is possible that the reduction in both microglial and astrocyte activation observed at 7 days post-ischemia with normoxic reperfusion contributes to improved long-term outcome; however, additional studies are necessary to support this hypothesis. Alternatively, the greater microglial and astrocyte activation observed at 7 days after hyperoxic reperfusion may simply be a consequence of greater ongoing cell death in this period.

In summary, while histological findings are supportive of the damaging effects of hyperoxic early reperfusion in this rat global cerebral ischemia model, the neurological findings fail

to demonstrate a clear effect. Nevertheless, the results of these long-term outcome experiments with male rats, taken together with our previous results from short-term outcome studies with female dogs, call into question the appropriateness of indiscriminate clinical use of 100% ventilatory oxygen immediately after cardiac arrest. This concern was also expressed by the International Liaison Committee on Resuscitation, stating that "On the basis of preclinical evidence alone, unnecessary arterial hyperoxia should be avoided, especially during the initial post-cardiac arrest period" (Neumar et al., 2008). Moreover, clinical studies indicate that normoxic resuscitation after neonatal asphyxiation improves outcome compared to that observed with hyperoxic resuscitation (Obladen, 2009; Rabi et al., 2007). Additional clinical trials will be necessary to determine if the results we have obtained with both small and large animal models of global cerebral ischemia and reperfusion apply to resuscitation following cardiac arrest in humans.

Acknowledgment

This work was supported by National Institutes of Health grants R01NS34152 and U01NS49425.

Author Disclosure Statement

No competing financial interests exist.

References

- Balan, I.S., Fiskum, G., Hazelton, J., Cotto-Cumba, C., and Rosenthal, R.E. (2006). Oximetry-guided reoxygenation improves neurological outcome after experimental cardiac arrest. *Stroke* 37, 3008–3013.
- Dietrich, W.D., Busto, R., Alonso, O., Globus, M.Y., and Ginsberg, M.D. (1993). Intraischemic but not postischemic brain hypothermia protects chronically following global forebrain ischemia in rats. *J. Cereb. Blood Flow Metab.* 13, 541–549.
- Feng, Z.C., Sick, T.J., and Rosenthal, M. (1998). Oxygen sensitivity of mitochondrial redox status and evoked potential recovery early during reperfusion in post-ischemic rat brain. *Resuscitation* 37, 33–41.
- Hailer, N.P. (2008). Immunosuppression after traumatic or ischemic CNS damage: it is neuroprotective and illuminates the role of microglial cells. *Prog. Neurobiol.* 84, 211–233.
- Liebeskind, D.S., and Kasner, S.E. (2001). Neuroprotection for ischaemic stroke: an unattainable goal? *CNS Drugs* 15, 165–174.
- Liu, Y., Rosenthal, R.E., Haywood, Y., Miljkovic-Lolic, M., Vanderhoek, J.Y., and Fiskum, G. (1998). Normoxic ventilation after cardiac arrest reduces oxidation of brain lipids and improves neurological outcome. *Stroke* 29, 1679–1686.
- Mickel, H.S., Kempfski, O., Feuerstein, G., Parisi, J.E., and Webster, H.D. (1990). Prominent white matter lesions develop in Mongolian gerbils treated with 100% normobaric oxygen after global brain ischemia. *Acta Neuropathol. (Berl.)* 79, 465–472.
- Mickel, H.S., Vaishnav, Y.N., Kempfski, O., Von Lubitz, D., Weiss, J.F., and Feuerstein, G. (1987). Breathing 100% oxygen after global brain ischemia in Mongolian gerbils results in increased lipid peroxidation and increased mortality. *Stroke* 18, 426–430.
- Neumar, R.W., Nolan, J.P., Adrie, C., Aibiki, M., Berg, R.A., Böttiger, B.W., Callaway, C., Clark, R.S., Geocadin, R.G., Jauch, E.C., Kern, K.B., Laurent, I., Longstreth, W.T. Jr., Merchant, R.M., Morley, P., Morrison, L.J., Nadkarni, V., Peberdy, M.A., Rivers, E.P., Rodriguez-Nunez, A., Sellke, F.W., Spaulding, C., Sunde, K., and Vanden Hoek, T. (2008). Post-cardiac arrest syndrome: epidemiology, pathophysiology, treatment, and prognostication. A consensus statement from the International Liaison Committee on Resuscitation (American Heart Association, Australian and New Zealand Council on Resuscitation, European Resuscitation Council, Heart and Stroke Foundation of Canada, InterAmerican Heart Foundation, Resuscitation Council of Asia, and the Resuscitation Council of Southern Africa); the American Heart Association Emergency Cardiovascular Care Committee; the Council on Cardiovascular Surgery and Anesthesia; the Council on Cardiopulmonary, Perioperative, and Critical Care; the Council on Clinical Cardiology; and the Stroke Council. *Circulation* 118, 2452–2483.
- Obladen, M. (2009). History of neonatal resuscitation. Part 2: oxygen and other drugs. *Neonatology* 95, 91–96.
- Olsen, G.M., Scheel-Kruger, J., Moller, A., and Jensen, L.H. (1994). Relation of spatial learning of rats in the Morris water maze task to the number of viable CA1 neurons following four-vessel occlusion. *Behav. Neurosci.* 108, 681–690.
- Rabi, Y., Rabi, D., and Yee, W. (2007). Room air resuscitation of the depressed newborn: a systematic review and meta-analysis. *Resuscitation* 72, 353–363.
- Richards, E.M., Fiskum, G., Rosenthal, R.E., Hopkins, I., and McKenna, M.C. (2007). Hyperoxic reperfusion after global ischemia decreases hippocampal energy metabolism. *Stroke* 38, 1578–1584.
- Richards, E.M., Rosenthal, R.E., Kristian, T., and Fiskum, G. (2006). Postischemic hyperoxia reduces hippocampal pyruvate dehydrogenase activity. *Free Radic. Biol. Med.* 40, 1960–1970.
- Rosenthal, R.E., Silbergleit, R., Hof, P.R., Haywood, Y., and Fiskum, G. (2003). Hyperbaric oxygen reduces neuronal death and improves neurological outcome after canine cardiac arrest. *Stroke* 34, 1311–1316.
- Schmitz, C., and Hof, P.R. (2000). Recommendations for straightforward and rigorous methods of counting neurons based on a computer simulation approach. *J. Chem. Neuroanat.* 20, 93–114.
- Singhal, A.B., Benner, T., Roccatagliata, L., Koroshetz, W.J., Schaefer, P.W., Lo, E.H., Buonanno, F.S., Gonzalez, R.G., and Sorensen, A. (2005). A pilot study of normobaric oxygen therapy in acute ischemic stroke. *Stroke* 36, 797–802.
- Skelton, R.W. (1998). Modelling recovery of cognitive function after traumatic brain injury: spatial navigation in the Morris water maze after complete or partial transections of the perforant path in rats. *Behav. Brain Res.* 96, 13–35.
- Smith, M.L., Auer, R.N., and Siesjo, B.K. (1984). The density and distribution of ischemic brain injury in the rat following 2–10 min of forebrain ischemia. *Acta Neuropathol. (Berl.)* 64, 319–332.
- Soltys, Z., Ziąja, M., Pawlinski, R., Setkowicz, Z., and Janeczko, K. (2001). Morphology of reactive microglia in the injured cerebral cortex. Fractal analysis and complementary quantitative methods. *J. Neurosci. Res.* 63, 90–97.
- Sugawara, T., Lewen, A., Noshita, N., Gasche, Y., and Chan, P.H. (2002). Effects of global ischemia duration on neuronal, astroglial, oligodendroglial, and microglial reactions in the vulnerable hippocampal CA1 subregion in rats. *J. Neurotrauma* 19, 85–98.
- Tolias, C.M., Reinert, M., Seiler, R., Gilman, C., Scharf, A., and Bullock, M.R. (2004). Normobaric hyperoxia-induced improvement in cerebral metabolism and reduction in intracranial

- pressure in patients with severe head injury: a prospective historical cohort-matched study. *J. Neurosurg.* 101, 435–444.
- Vereczki, V., Martin, E., Rosenthal, R.E., Hof, P.R., Hoffman, G.E., and Fiskum, G. (2006). Normoxic resuscitation after cardiac arrest protects against hippocampal oxidative stress, metabolic dysfunction, and neuronal death. *J. Cereb. Blood Flow Metab.* 26, 821–835.
- Watson, R.E., Jr., Wiegand, S.J., Clough, R.W., and Hoffman, G.E. (1986). Use of cryoprotectant to maintain long-term peptide immunoreactivity and tissue morphology. *Peptides* 7, 155–159.
- West, M.J., Slomianka, L., and Gundersen, H.J. (1991). Unbiased stereological estimation of the total number of neurons in the subdivisions of the rat hippocampus using the optical fractionator. *Anat. Rec.* 231, 482–497.
- Whishaw, I.Q., Rod, M.R., and Auer, R.N. (1994). Behavioral deficits revealed by multiple tests in rats with ischemic damage limited to half of the CA1 sector of the hippocampus. *Brain Res. Bull.* 34, 283–289.
- Williams, J.A., Barreiro, C.J., Nwakanma, L.U., Lange, M.S., Kratz, L.E., Blue, M.E., Berrong, J., Patel, N.D., Gott, V.L., Troncoso, J.C., Johnston, M.V., and Baumgartner, W.A. (2006). Valproic acid prevents brain injury in a canine model of hypothermic circulatory arrest: a promising new approach to neuroprotection during cardiac surgery. *Ann. Thorac. Surg.* 81, 2235–2241.
- Zwemer, C.F., Whitesall, S.E., and D'alecy, L.G. (1994). Cardiopulmonary-cerebral resuscitation with 100% oxygen exacerbates neurological dysfunction following nine minutes of normothermic cardiac arrest in dogs. *Resuscitation* 27, 159–170.

Address correspondence to:

Gary Fiskum, Ph.D.

Department of Anesthesiology

University of Maryland–Baltimore

MSTF 5.34

685 W. Baltimore Street

Baltimore, MD 21201

E-mail: gfiskum@anes.umm.edu